Journal of Geriatric Cardiology (2019) 16: 540–551

Research Article · Open Access ·

Effects of febuxostat on atrial remodeling in a rabbit model of atrial fibrillation induced by rapid atrial pacing

Yong-Yan FAN[1,2,*], Feng XU[3,*], Chao ZHU[4], Wen-Kun CHENG[2], Jian LI[2], Zhao-Liang SHAN[2], Yang LI[2,#], Yu-Tang WANG[1,5,#]

[1]*College of Medicine, Nankai University, Tianjin, China*
[2]*Department of Cardiology, Chinese PLA General Hospital, Beijing, China*
[3]*Department of Bone & Joint, Shijingshan Teaching Hospital of Capital Medical University, Beijing Shijingshan Hospital, Beijing, China*
[4]*Department of Heart Center, Beijing Friendship Hospital, Capital Medical University, Beijing, China*
[5]*Department of Geriatric Cardiology, Chinese PLA General Hospital, Beijing, China*

Abstract

Background Febuxostat, a novel nonpurine selective inhibitor of xanthine oxidase (XO), may be used in the prevention and management of atrial fibrillation (AF). The purpose of this study was to evaluate the effects of febuxostat on atrial remodeling in a rabbit model of AF induced by rapid atrial pacing (RAP) and the mechanisms by which it acts. **Methods** Twenty-four rabbits were randomly divided into four groups: sham-operated group (Group S), RAP group (Group P), RAP with 5 mg/kg per day febuxostat group (Group LFP), and RAP with 10 mg/kg per day febuxostat group (Group HFP). All rabbits except those in Group S were subjected to RAP at 600 beats/min for four weeks. The effects of febuxostat on atrial electrical and structural remodeling, markers of inflammation and oxidative stress, and signaling pathways involved in the left atrium were examined. **Results** Shortened atrial effective refractory period (AERP), increased AF inducibility, decreased mRNA levels of Cav1.2 and Kv4.3, and left atrial enlargement and dysfunction were observed in Group P, and these changes were suppressed in the groups treated with febuxostat. Prominent atrial fibrosis was observed in Group P, as were increased levels of TGF-β1, Collagen I, and α-SMA and decreased levels of Smad7 and eNOS. Treatment with febuxostat attenuated these differences. Changes in inflammatory and oxidative stress markers induced by RAP were consistent with the protective effects of febuxostat. **Conclusions** This study is the first to find that febuxostat can inhibit atrial electrical and structural remodeling of AF by suppressing XO and inhibiting the TGF-β1/Smad signaling pathway.

J Geriatr Cardiol 2019; 16: 540–551. doi:10.11909/j.issn.1671-5411.2019.07.003

Keywords: Atrial fibrillation; Atrial remodeling; Febuxostat; Rapid atrial pacing; Xanthine oxidase

1 Introduction

Atrial fibrillation (AF) is the most common form of sustained cardiac arrhythmia encountered in clinical practice, and it is associated with an increased risk of stroke, systemic embolism, heart failure, hospitalization, and death.[1] Current therapeutic approaches to AF, including pharmacological treatment and catheter ablation, have limited efficacy and potentially adverse effects.[2] Despite extensive studies, the pathophysiology of AF is not well established.[3] Ectopic firing and reentry can promote and maintain AF, and both have been found to be related to atrial electrical and structural remodeling.[3,4] Atrial fibrosis, a hallmark of atrial structural remodeling, plays a critical role in the maintenance of chronic AF,[3] but the mechanisms responsible for atrial fibrosis and the underlying signaling pathways are still poorly understood.

Recent studies have found that inflammation and oxidative stress have a major impact on atrial structural and electrical remodeling and may promote the pathogenesis of AF.[5,6] Inflammatory cell infiltration and calcium overload during periods of high atrial rate in AF may promote oxidative damage in atrial tissue, subsequently promoting atrial fibrosis and facilitating the progression of AF.[7] The primary sources of reactive oxygen species (ROS) in atrial

[*]The first two authors contributed equally to this manuscript.

[#]**Correspondence to:** Yu-Tang WANG, College of Medicine, Nankai University, 94 Weijin Rd., Tianjin 300071, China; Department of Geriatric Cardiology, Chinese PLA General Hospital, 28 Fuxing Rd., Beijing 100853, China; Yang LI, Department of Cardiology, Chinese PLA General Hospital, 28 Fuxing Rd., Beijing 100853, China. E-mails: wangyutang2017@163.com (WANG YT); liyangbsh@sina.com (LI Y).

Received: March 27, 2019 **Revised:** June 6, 2019
Accepted: June 24, 2019 **Published online:** July 28, 2019

tissue are the mitochondrial electron transport chain, xanthine oxidase (XO), uncoupled nitric oxide synthase (NOS) and nicotinamide adenine dinucleotide phosphate (NADPH) oxidases.[8] XO is believed to play a critical role in redox signaling in a wide range of cardiovascular disorders, particularly in AF.[9–14]

Xanthine oxidoreductase (XOR) is a major source of ROS in the cardiovascular system, and it is a key enzyme in uric acid (UA) metabolism.[15] XOR consists of two interconvertible forms: xanthine dehydrogenase (XDH) and XO. Under physiological conditions, the enzyme exists primarily as XDH, and it functions as a dehydrogenase with NAD^+ as an electron acceptor.[16] After oxidation of critical cysteines or partial cleavage of the enzyme, XDH converts to XO and facilitates the transfer of one and two electrons onto oxygen.[15] XO catabolizes purines by oxidizing hypoxanthine to UA with xanthine as an intermediate while producing superoxide anions and hydrogen peroxide, thus contributing to oxidative stress.[15,16] The interaction between XO and XDH plays an important role in the initiation and propagation of inflammatory and oxidative stress responses, thereby contributing to atrial remodeling and AF.

Allopurinol is a nonspecific XO inhibitor.[15] Sakabe, *et al*.[14] reported that allopurinol can suppress AF promotion in a canine model of atrial pacing-induced left ventricular dysfunction by preventing both electrical and structural remodeling, and they suggested that XO may play an important role in the enhancement of atrial vulnerability and might be a novel target of AF therapy. However, they did not determine the details of the mechanisms underlying the effects of allopurinol in that study. Febuxostat, a novel nonpurine selective inhibitor of XO, has greater bioavailability and a more potent XO-inhibitory effect than allopurinol.[17] It inhibits both the oxidized and reduced forms of the enzyme and inhibits the formation of ROS and the inflammation promoted by oxidative stress.[18,19] Evidence suggests that febuxostat exerts antioxidant effects by directly scavenging ROS.[11,13,18,20] Animal data have also shown febuxostat to be beneficial in chronic heart failure (CHF), myocardial ischemia/reperfusion injury, chronic kidney disease (CKD), and intestinal ischemia.[11,18,21,22] Hence, febuxostat could be suitable for use in the prevention and management of AF. Currently, the effects of febuxostat on atrial remodeling, as well as the potential mechanisms by which it could modulate atrial remodeling, have yet to be studied and are poorly understood. The purpose of this study was to evaluate the effects of febuxostat on atrial electrical and structural remodeling in a rabbit model of AF induced by rapid atrial pacing (RAP) and to investigate the mechanisms underlying the potential protective effects of febuxostat.

2 Methods

2.1 Animal preparation

All animals used in this study received humane care in compliance with the Guiding Principles for the Care and Use of Animals in the Field of Physiological Sciences and followed the Chinese guidelines for experimental animals. The protocols and care of experimental rabbits were supervised and approved by the Animal Ethical Committee of the Chinese People's Liberation Army General Hospital.

2.2 Experimental design

Twenty-four male New Zealand white rabbits (3.0–3.5 kg) were purchased from the Experimental Animal Department of the Chinese People's Liberation Army General Hospital. The rabbits were randomly divided into four groups (n = 6/group): sham-operated group (Group S), RAP group (Group P), RAP with 5 mg/kg per day febuxostat group (Group LFP), and RAP with 10 mg/kg per day febuxostat group (Group HFP). The rabbits were anesthetized with an intravenous injection of 3% pentobarbital sodium (30 mg/kg) via the marginal ear vein. Rabbits were not mechanically ventilated and were allowed to breathe 100% oxygen on their own during the surgery. Heart rhythms were monitored using a limb lead ECG. The left thoracic cavity was opened via the third intercostal space, and the heart was exposed by a dilator. The pericardium was opened gently, and the electrode was placed and sutured to the free wall of the left atrial appendage. The distal end of the electrode lead was tunneled subcutaneously and connected to a programmable pacemaker (Lepu Medical Technology Co., Ltd, Shanghai, China) implanted in a subcutaneous pocket in the abdomen of the rabbit. When surgery was completed, the rabbits were given antibiotics and allowed to recover for one week.

After recovery, the pacemaker (AOO pacing mode, output of 2.7 V with 0.37 ms pulse duration) was programmed to provide RAP at 600 beats/min for four weeks. Rabbits in Group S were operated on with an identical surgery procedure, excluding RAP. During the period of RAP, their ECG was measured every day to ensure that the pacemaker was working properly, and febuxostat (Wanbang Biochemical Pharmaceutical Co., Ltd., Jiangsu, China) was given daily by oral administration until RAP was ended. The febuxostat oral dose of 10 mg/kg was estimated to provide a similar plasma level of febuxostat to the clinically efficacious dose, and the dose was comparable to human doses used for the treatment of hyperuricemia, pharmacologically scaled for rabbits. Rabbits in Group S and Group P received an equal amount of oral placebo.

2.3 Electrophysiological studies

Electrophysiological studies were performed before and after four weeks of RAP to evaluate the effect of pacing on the electrophysiological properties of the left atrium (LA). These studies were performed as previously described.[13,23] A distal quadripolar pacing electrode (Medtronic Inc., Minneapolis, MN, USA) was firmly attached to the free wall of the left atrial appendage. A Jinjiang multichannel physiology recorder (LEAD-7000, Sichuan Jinjiang Electronic Science and Technology Co., Ltd, Sichuan, China) was used to deliver a 2-fold threshold current with a pulse width of 2 ms. The atrial effective refractory period (AERP) was measured at a basic cycle length of 200 ms with a train of 8 basic stimuli (S1), followed by a premature extra stimulus (S2). The S1-S2 intervals were decreased in 5 ms steps until S2 failed to produce the atrial response, then increased by 10 ms, and finally decreased in 2 ms steps until S2 failed to capture. The longest S1-S2 interval that failed to capture was defined as the AERP200. The mean value of three AERP200 measurements was used for data analysis. The inducibility of AF was tested by burst pacing 10 times (3-fold threshold current, cycle length 60 ms, duration 10 s) using a stimulator (DF-5A, Suzhou Dongfang Electronic Instruments Plant, Jiangsu, China). AF was defined as a rapid, irregular atrial rhythm with a duration longer than 1000 ms. AF inducibility was defined as the percentage of successful inductions of AF.

2.4 Echocardiography

Transthoracic echocardiographic examinations (ACUSON SC2000, Siemens, Malvern, PA, USA) were performed after four weeks of RAP to evaluate the structure and function of the LA and left ventricle (LV). Rabbits were anesthetized using xylazine hydrochloride injection (4 mg/kg) (Huamu Animal Health Products Co., Ltd, Jilin, China) administered intramuscularly, and the anterior chest area of the rabbits was shaved. The rabbits were placed on a table in the left lateral decubitus position, and two-dimensional images and M-mode tracings were recorded. Echocardiographic measurements included left atrial anteroposterior diameter (LAD), left ventricular posterior wall thickness (LVPWT), interventricular septal thickness (IVST), left ventricular end-diastolic dimension (LVEDD), left ventricular end-systolic dimension (LVESD), and left ventricular ejection fraction (LVEF). Left atrial maximum volume (LAV_{max}) was recorded immediately before the mitral valve opening. The left atrial minimum volume (LAV_{min}) was recorded at the peak of the R wave of the simultaneously recorded electrocardiogram. Left atrial total ejection fraction (LAEF) was calculated as (LAV_{max}–LAV_{min})/LAV_{max}.

2.5 Sample preparation

At the end of the experiment, the rabbits were euthanized by an intravenous overdose of 3% pentobarbital sodium (100 mg/kg). Blood samples were collected from the jugular vein, and left atrial tissues were excised and divided into several portions. Blood samples were centrifuged at 3000 × g for 15 min at 4°C, and supernatants were collected to measure the serum parameters. The left atrial tissues were harvested, cut into 1 mm^3 sections on ice, and fixed with 2.5% glutaraldehyde for transmission electron microscopy. To prepare myocardial homogenates for further biochemical analysis, left atrial tissues were collected, weighed, and homogenized in phosphate-buffered saline (PBS, pH = 7.4; 1 g tissue per 9 mL PBS) using a tissue homogenizer (Ultra-Turrax® T25 basic, IKA®-Werke, Staufen, Germany). After centrifugation at 15,000 × *g* for 10 min at 4°C, the supernatants were collected and stored at −80°C until analysis. One portion of the left atrial tissue from each rabbit was fixed in 10% phosphate-buffered formalin and embedded in paraffin for morphologic analyses by light microscopy. The remainder of each left atrial sample was snap-frozen in liquid nitrogen and stored at −80°C for subsequent RNA and protein extraction.

2.6 Analysis of oxidative stress in left atrial homogenates

Left atrial homogenates were used to estimate superoxide dismutase (SOD) activity and the levels of XO and XDH in left atrial tissues. Commercially available sandwich enzyme-linked immunosorbent assay (ELISA) kits (EXPANDBIO Technology Co., Ltd, Beijing, China) were used according to the manufacturer's instructions.

2.7 Measurement of serum inflammatory and cardiac remodeling parameters

Serum levels of high-sensitivity C-reactive protein (hs-CRP), growth differentiation factor-15 (GDF-15), and galectin-3 were assayed with sandwich ELISA kits (EXPANDBIO Technology Co., Ltd, Beijing, China).

2.8 Hematoxylin–eosin staining and Masson's trichrome staining

Left atrial tissue was fixed in 10% phosphate-buffered formalin, embedded in paraffin, sliced into 4 μm serial sections, and subjected to pathological examination following hematoxylin-eosin (H&E) staining and Masson's trichrome staining. Photomicrographs were obtained using an Olympus BX53 microscope (Olympus, Tokyo, Japan). Masson's

trichrome staining was used to evaluate atrial interstitial fibrosis. The collagen fibers are marked with blue, while the cardiomyocytes are marked with red. Semiquantitative analysis of the proportion of collagen fibers was conducted using the Image-Pro Plus 6.0 image analysis system (Media Cybernetics, Maryland, USA). The proportion of fibrous tissue area was calculated by the following equation: collagen fiber area/total view area 100%.

2.9 Transmission electron microscopy

One portion of the left atrial tissue was cut into 1-mm^3 sections, fixed with 2.5% glutaraldehyde, rinsed with sucrose buffer, and refixed with 1% osmic acid. Samples were then dehydrated with a series of ethanol rinses and sliced into 60 nm serial sections. The slices were stained, and the ultrastructure of the myocardium was observed using a Philips CM 120 transmission electron microscope (Philips, Amsterdam, Netherlands).

2.10 Western blot analysis of TGF-β1, Smad7, eNOS, Collagen I, and α-SMA

Left atrial tissue was homogenized in lysis buffer containing radioimmunoprecipitation assay (RIPA) buffer and inhibitors of proteases. Protein concentrations were determined by the bicinchoninic acid (BCA) assay. Proteins were separated by SDS-polyacrylamide gel electrophoresis (SDS-PAGE), with 8% gels used for endothelial nitric oxide synthase (eNOS) and Collagen I and 10% gels used for TGF-β1, Smad7, and α-SMA. The fractionated proteins were electrophoretically transferred to nitrocellulose membranes (Amersham, Piscataway, NJ, USA). The membranes were incubated with the appropriate primary antibodies for each target protein at 4°C overnight. The primary antibodies for TGF-β1 (1: 500), eNOS (1: 500), Collagen I (1: 500), and α-SMA (1: 200) were from Abcam (Cambridge, MA, USA). The Smad7 (1: 1000) primary antibody was from Aviva Systems Biology (San Diego, CA, USA). The secondary antibodies for Smad7 and eNOS were horseradish peroxidase (HRP)-conjugated goat anti-rabbit IgG (Abcam), diluted 1: 5000. The secondary antibodies for TGF-β1, Collagen I, and α-SMA were HRP-conjugated goat anti-mouse IgG (Abcam), diluted 1:5000. Stained bands were visualized after incubation with HRP-conjugated secondary antibody using enhanced chemiluminescence (ECL) detection reagents (Amersham). GAPDH (1: 2500; Solarbio, Beijing, China) was used as a loading control.

2.11 Quantitative real-time PCR assay for Cav1.2, Kv4.3, TGF-β1, Smad7, eNOS, Collagen I, and α-SMA

Total RNA was extracted using the TRIZOL reagent (Invitrogen, Carlsbad, CA, USA) following the manufacturer's protocol, and cDNA was synthesized using a cDNA Synthesis Kit (Fermentas International Inc., Burlington, Ontario, Canada) following the manufacturer's instructions. After reverse-transcription, cDNA samples were subjected to polymerase chain reaction (PCR) amplification. For real-time assays, PCRs were prepared in SYBR Green Supermix (Toyobo, Ltd, Tokyo, Japan). Each PCR was performed in triplicate in a final volume of 20 μL, containing 10 μL SYBR Green dye, 1 μL diluted cDNA, 0.2 μM of each paired primer, and 8.6 μL deionized water. The PCR protocol was as follows: initial denaturation for 15 min at 95°C, 40 cycles of denaturation for 15 s at 95°C, and extension for 30 s at 60°C. Specific primers were designed for each mRNA sequence of interest. Threshold cycle (Ct) values for Cav1.2, Kv4.3, TGF-β1, Smad7, eNOS, Collagen I, and α-SMA were measured, and the values were normalized to those of GAPDH and are expressed as relative ratios. Data analysis was carried out using the $2^{-\Delta\Delta Ct}$ method for each gene. Primer sequences are listed in Table 1.

2.12 Statistical analysis

Statistical evaluation was performed with SPSS 19.0 (Statistical Packages for Social Sciences; SPSS Inc., Chicago, Illinois, USA). Data with normal distributions are presented as means ± SD, and categorical variables are expressed as percentages. Prism 7.0 (GraphPad, San Diego, CA, USA) was used for statistical analyses and to generate

Table 1. Sequences of the primers used for quantitative real-time PCR.

Genes	Forward	Reverse
Cav1.2	5′-GCTGTGTCTGCTGCCTCTGAAG-3′	5′-TCGGTGTCGCCTTGGTTGTTG-3′
Kv4.3	5′- ATCATTGGCGACTGCTGCTACG-3′	5′-CGGCATGGACTCCTGGTTGTTC-3′
TGF-β1	5′-AGCTGTACATTGACTTCCGCAAGG-3′	5′-CAGGCAGAAGTTGGCGTGGTAG-3′
Smad7	5′-CTCGGAAGTCAAGAGGCTGTGTTG-3′	5′-TCTAGTTCGCAGAGTCGGCTAAGG-3′
eNOS	5′-ACATCACCTCTCCATCCAGTCCTC-3′	5′-ACCACTTCCACTCCTCGTAGCG-3′
Collagen I	5′-TTGCTTGAAGACCCGAGTGG-3′	5′-TTGGTTGCTGGCAGGACAAT-3′
α-SMA	5′-CATTGTGCTGGACTCTGGAGATGG-3′	5′-CCACGCTCAGTCAGGATCTTCATG-3′
GAPDH	5′-TCTACCTTCGATGCTGGGGC-3′	5′-TCTCGTCCTCCTCTGGTGCT-3′

figures. Statistical significance was assessed using one-way analysis of variance (ANOVA) with post hoc analysis by Tukey's test for multiple comparisons. The Pearson chi-square test was used to compare the inducibility of AF between the baseline and after four weeks of RAP. A value of $P < 0.05$ was considered statistically significant.

3 Results

3.1 Effects of febuxostat on AERP and the inducibility of AF

The ECG recordings of the rabbits during electrophysiology studies are shown in Figure 1. These ECG recordings showed that RAP caused the disappearance of P waves and induced irregular RR intervals, which are typical signs of sustained AF. The changes between AERP 200 at baseline and AERP 200 after four weeks of RAP in rabbits are shown in Figure 2A and B, respectively. The effects of febuxostat on the inducibility of AF are shown in Figure 2C. The sham operation had no effect on the AERP200 or the inducibility of AF. Under baseline conditions, there was no significant difference in AERP 200 among the four groups ($P > 0.05$). After 4 weeks of RAP, AERP 200 was significantly reduced in Group P compared to Group S (73.53 ± 5.06 *vs*. 93.75 ± 6.22, $P < 0.01$). In contrast, treatment with febuxostat (10 mg/kg per day) resulted in a significant increase in AERP 200 compared to Group P (85.02 ± 5.35 *vs*. 73.53 ± 5.06, $P < 0.01$). Moreover, RAP significantly increased AF inducibility compared to the baseline conditions in Group P (58.3% *vs*. 8.3%, $P < 0.01$), Group LFP (43.3% *vs*. 11.7%, $P < 0.01$), and Group HFP (35.0% *vs*. 15.0%, $P = 0.011$), but not in Group S (16.7% *vs*. 10.0%, $P = 0.283$). After treatment with febuxostat, the inducibility of AF was reduced to a certain extent compared to the baseline conditions, especially in Group HFP.

3.2 Effects of febuxostat on atrial ion-channel remodeling

To investigate whether RAP affected the activities of ion channels in the LA, qRT-PCR was used to quantitatively determine the mRNA levels of Cav1.2 and Kv4.3. As shown in Figure 2D, Cav1.2 mRNA level was significantly decreased in Group P compared with Group S ($P < 0.01$). However, treatment with febuxostat significantly increased the expression of Cav1.2 compared to Group P, especially at

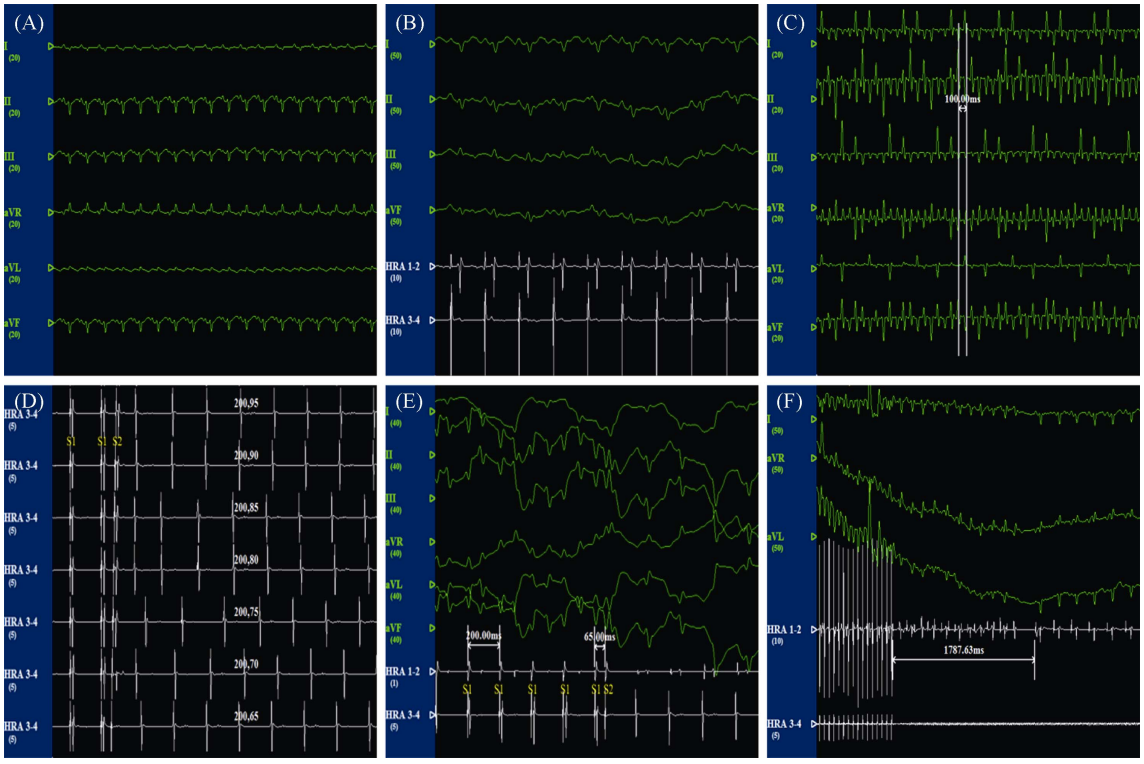

Figure 1. ECG recordings of rabbits during electrophysiology studies. (A): The ECG of limb leads under the normal state; (B): the ECG of limb leads and the potential of the left atrium under the normal state; (C): the ECG of limb leads during rapid atrial pacing at 600 beats/min; (D): intracardiac electrophysiological examination and S1-S2 programmed stimulation; (E): AERP measurement. S2 (stimulate interval = 65 ms) was unable to induce a propagated atrial response; and (F): representative atrial fibrillation episode induced by high-frequency atrial burst pacing at 1000 beats/min. AERP: atrial effective refractory period.

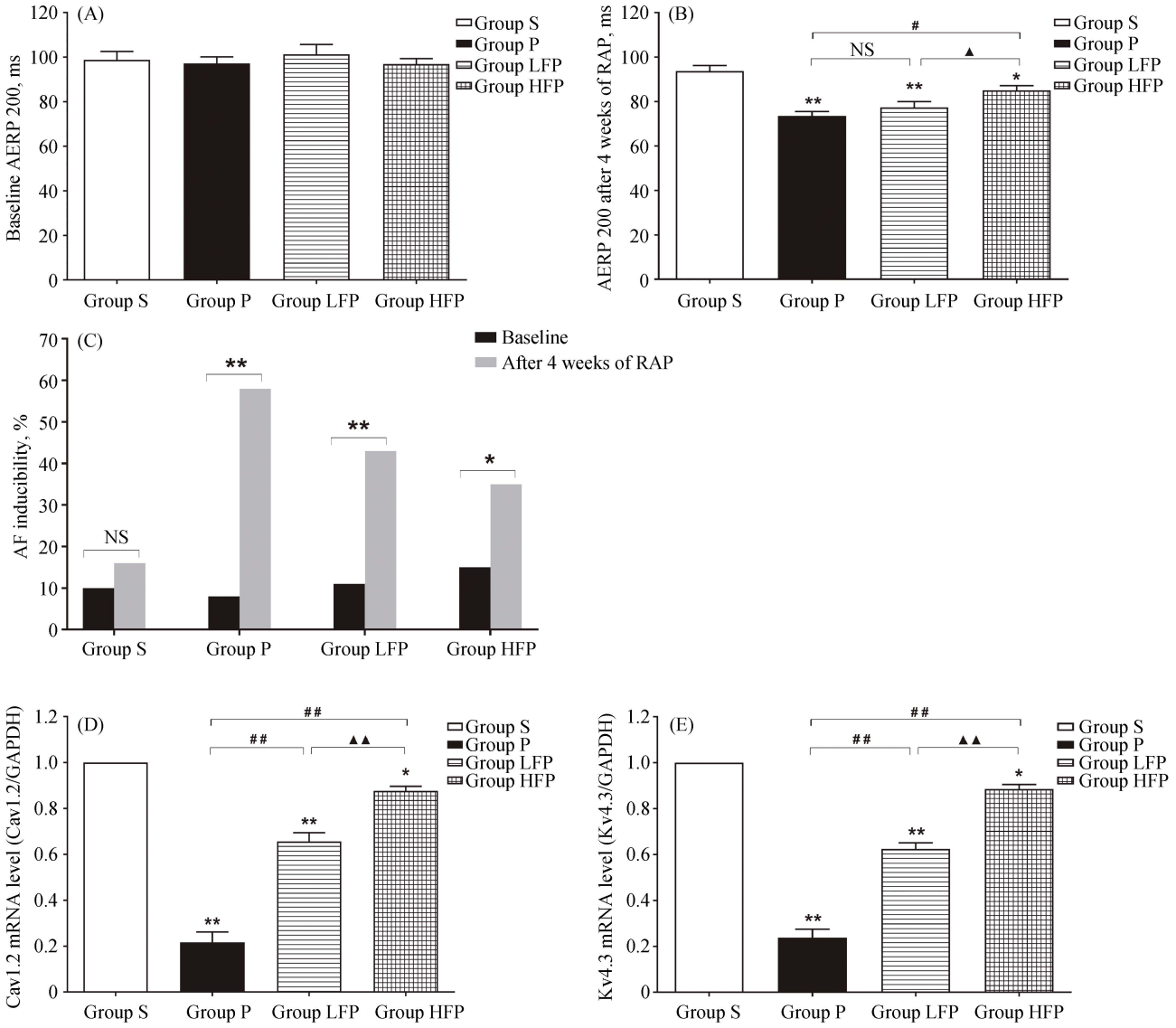

Figure 2. Effects of febuxostat on atrial electrical remodeling. (A): Baseline AERP200 in the four groups; (B): AERP200 after four weeks of RAP in the four groups; (C): effects of febuxostat on the inducibility of AF; (D): quantitative analysis of the mRNA expression of Cav1.2 in the four groups; and (E): quantitative analysis of the mRNA expression of Kv4.3 in the four groups. Values are expressed as means ± SD (n = 6/group); $^{*}P < 0.05$ and $^{**}P < 0.01$ *vs*. Group S; $^{\#}P < 0.05$, $^{\#\#}P<0.01$ *vs*. Group P; $^{\blacktriangle}P < 0.05$, $^{\blacktriangle\blacktriangle}P < 0.01$ *vs*. Group LFP. Group HFP: RAP with 10 mg/kg per day febuxostat group; Group LFP: RAP with 5 mg/kg per day febuxostat group; Group P: RAP group; Group S: sham-operated group. AERP: atrial effective refractory period; AF: atrial fibrillation; NS: not significant; RAP: rapid atrial pacing.

a dose of 10 mg/kg per day (0.88 ± 0.03 *vs*. 0.22 ± 0.08, $P <$ 0.01). As shown in Figure 2E, Kv4.3 mRNA level was also significantly decreased in Group P compared to Group S (P < 0.01), and this downregulation was prevented in febuxostat-treated groups ($P < 0.01$).

3.3 Effects of febuxostat on atrial structural remodeling

H&E staining was performed to observe pathological alterations in myocardial histomorphology (Figure 3A). Left atrial tissue from Group S appeared to be normal. However, left atrial tissue from Group P was found to have serious pathological damage, and H&E staining showed swollen myocardial fibres, a disappearance in horizontal stripes, disordered atrial muscle arrangement, wider spaces between branches, and even cardiomyocyte lysis and necrosis. Treatment with febuxostat was found to attenuate these abnormal pathological changes, and a dose of 10 mg/kg per day seemed to have a more robust protective effect than does a dose of 5 mg/kg per day.

As shown in Figure 3B and C, RAP resulted in a marked

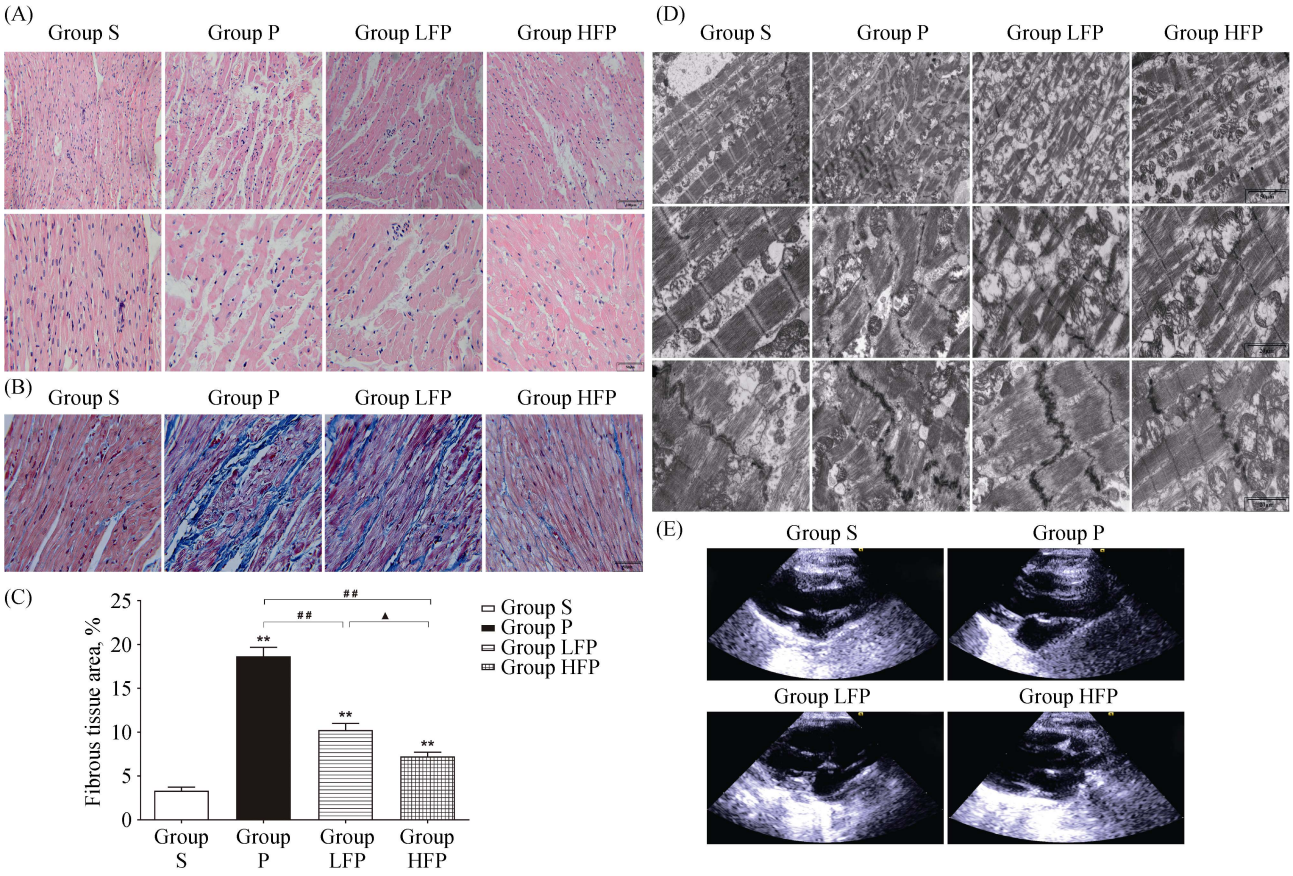

Figure 3. Effects of febuxostat on atrial structural remodeling. (A): Representative images showing H&E staining in tissues from the four groups; (B): representative images showing Masson's trichrome staining in tissues from the four groups; (C): semiquantitative analysis of the proportion of fibrous tissue area in the four groups; (D): representative transmission electron micrographs of left atrial ultrastructure in the four groups; and (E): representative echocardiographic images of the left atrium in the four groups. Values are expressed as means ± SD (n = 6 per group); $^{**}P < 0.01$ *vs.* Group S; $^{\#\#}P < 0.01$ *vs.* Group P; $^{\blacktriangle\blacktriangle}P < 0.01$ *vs.* Group LFP. Group HFP: RAP with 10 mg/kg per day febuxostat group; Group LFP: RAP with 5 mg/kg per day febuxostat group; Group P: RAP group; Group S: sham-operated group. 200 × magnification, bar = 100 μm; 400 × magnification, bar = 50 μm; 2000× magnification, bar = 50 μm; 5000 × magnification, bar = 20 μm. RAP: rapid atrial pacing.

deposition of collagen in the LA, as estimated by Masson's trichrome staining. Left atrial tissue from Group S displayed grossly normal atria with a small amount of interstitial fibrosis, in contrast to the substantial interstitial fibrosis observed in tissue from Group P. Furthermore, the proportion of fibrous tissue area in Group P was significantly higher than that in Group S (18.66% ± 2.51% *vs.* 3.33% ± 0.98%, $P < 0.01$), which was found to be partially suppressed by treatment with febuxostat, especially at a dose of 10 mg/kg per day.

As shown in Figure 3D, the myocardial fibers in Group S were arranged regularly, with an intact Z-band, a small amount of collagen deposition, and a clear structure of the intercalated disc. However, RAP induced mitochondrial structural disruption, including swelling, rupture, and loss of cristae. Furthermore, in Group P, the arrangement of myocardial fibers was disordered, the Z-band disappeared, there were high levels of collagen fiber deposition, the intercalated disc was twisted and dilated, and some of the gap junctions of the intercalated disc disappeared. By contrast, treatment with febuxostat reduced the degree of mitochondrial swelling and ameliorated the ultrastructural impairment of the LA, and this was especially apparent in Group HFP.

Figure 3E shows representative echocardiographic images of the LA after 4 weeks of RAP. Table 2 summarizes the changes in the echocardiographic parameters. LAD, LAV_{max}, and LAV_{min} were significantly increased in Group P compared to those in Group S ($P < 0.01$), whereas LAEF was dramatically decreased ($P < 0.01$). These changes were partially suppressed by treatment with febuxostat (10 mg/kg per day) ($P < 0.05$). Although LA enlargement and

Table 2. Effects of febuxostat on echocardiographic indices after four weeks of RAP.

Index	Group S	Group P	Group LFP	Group HFP
LAD, mm	9.22 ± 0.17	12.95 ± 0.44**	11.73 ± 0.42$^{**\#\#}$	10.65 ± 0.45$^{**\#\#\blacktriangle\blacktriangle}$
LAV_{max}, mL	0.99 ± 0.14	2.13 ± 0.15**	1.94 ± 0.20$^{**\#}$	1.92 ± 0.09$^{**\#}$
LAV_{min}, mL	0.52 ± 0.08	1.29 ± 0.12**	1.16 ± 0.11$^{**\#}$	1.14 ± 0.08$^{**\#}$
LAEF, %	47.89 ± 2.03	39.37 ± 3.93**	41.86 ± 2.32**	43.08 ± 2.38$^{**\#}$
LVPWT, mm	2.30 ± 0.42	2.77 ± 0.71	2.50 ± 0.45	2.38 ± 0.49
IVST, mm	2.30 ± 0.53	2.57 ± 0.52	2.45 ± 0.33	2.35 ± 0.58
LVEDD, mm	13.47 ± 1.05	15.88 ± 1.51**	15.11 ± 1.04*	13.90 ± 0.83$^{\#\#}$
LVESD, mm	8.01 ± 0.91	10.37 ± 1.81**	9.74 ± 1.50*	9.22 ± 0.98
LVEF, %	75.57 ± 4.64	72.87 ± 3.89	73.60 ± 2.88	74.32 ± 3.32

Values are expressed as means ± SD (n = 6/group); $^{*}P < 0.05$ and $^{**}P < 0.01$ *vs*. Group S; $^{\#}P < 0.05$ and $^{\#\#}P < 0.01$ *vs*. Group P; $^{\blacktriangle\blacktriangle}P < 0.01$ *vs*. Group LFP. Group HFP: RAP with 10 mg/kg per day febuxostat group; Group LFP: RAP with 5 mg/kg per day febuxostat group; Group P: RAP group; Group S: sham-operated group. IVST: interventricular septal thickness; LAD: left atrial anteroposterior diameter; LAEF: left atrial total ejection fraction; LAV_{max}, left atrial maximum volume; LAV_{min}: left atrial minimum volume; LVPWT: left ventricular posterior wall thickness; LVEDD: left ventricular end-diastolic dimension; LVESD: left ventricular end-systolic dimension; RAP: rapid atrial pacing.

Table 3. Effects of febuxostat on the levels of SOD, XO, XDH, hs-CRP, GDF-15, and galectin-3.

Index	Group S	Group P	Group LFP	Group HFP
SOD, U/L	186.16 ± 10.13	131.49 ± 9.07**	150.53 ± 5.41$^{**\#\#}$	168.33 ± 6.91$^{**\#\#\blacktriangle\blacktriangle}$
XO, U/L	31.83 ± 2.90	46.00 ± 5.28**	40.45 ± 2.39$^{**\#}$	37.23 ± 2.22$^{*\#\#}$
XDH , U/L	17.66 ± 3.20	31.08 ± 2.18**	27.41 ± 2.26**	22.70 ± 2.88$^{*\#\#\blacktriangle}$
hs-CRP, μg/mL	4.38 ± 0.93	8.72 ± 0.87**	7.27 ± 0.40$^{**\#\#}$	6.34 ± 0.29$^{**\#\#\blacktriangle}$
GDF-15, ng/L	45.29 ± 4.06	80.91 ± 4.50**	69.97 ± 5.54$^{**\#\#}$	59.30 ± 5.02$^{**\#\#\blacktriangle\blacktriangle}$
Galectin-3, ng/L	4464.94 ± 193.54	8758.40 ± 429.72**	7148.76 ± 261.78$^{**\#\#}$	6050.48 ± 516.72$^{**\#\#\blacktriangle\blacktriangle}$

Values are expressed as means ± SD (n = 6 per group); $^{*}P < 0.05$ and $^{**}P < 0.01$ *vs*. Group S; $^{\#}P < 0.05$ and $^{\#\#}P < 0.01$ *vs*. Group P; $^{\blacktriangle}P < 0.05$ and $^{\blacktriangle\blacktriangle}P < 0.01$ *vs*. Group LFP. Group HFP: RAP with 10 mg/kg per day febuxostat group; Group LFP: RAP with 5 mg/kg per day febuxostat group; Group S: Sham-operated group; Group P: RAP group. GDF-15: growth differentiation factor-15; hs-CRP: high-sensitivity C-reactive protein; RAP: rapid atrial pacing; SOD: superoxide dismutase; XDH: xanthine dehydrogenase; XO: xanthine oxidase;.

dysfunction were observed after four weeks of RAP, no significant differences in LVPWT, IVST, or LVEF were found among the four groups. Moreover, there was an increase in LVEDD and LVESD after four weeks of RAP in Group P compared to Group S, while there were no significant differences between Group S and Group HFP. Furthermore, no statistically significant differences were found in these echocardiographic indices except in LAD between Group LFP and Group HFP. However, Group HFP had results closer in value to those observed in Group S than in those observed in Group LFP.

3.4 Effects of febuxostat on oxidative stress and inflammatory and cardiac remodeling parameters

As shown in Table 3, myocardial SOD activity in Group P was significantly lower than that in Group S ($P < 0.01$), while the levels of myocardial XO and XDH were significantly higher ($P < 0.01$). Treatment with febuxostat (10 mg/kg per day) increased myocardial SOD activity ($P < 0.01$) and decreased the levels of myocardial XO and XDH compared to Group P ($P < 0.01$). Furthermore, serum levels of hs-CRP, GDF-15, and galectin-3 were significantly increased in Group P compared to Group S ($P < 0.01$). However, the activities of serum hs-CRP, GDF-15, and galectin-3 in groups treated with febuxostat, particularly Group HFP, decreased significantly compared to in Group P ($P < 0.01$).

3.5 Effects of febuxostat on signal transduction pathways involved in atrial remodeling

To investigate the molecular mechanisms underlying the effects that febuxostat treatment has on atrial remodeling, the classic TGF-β1/Smad signal transduction pathway was examined. As shown in Figure 4, the mRNA and protein levels of TGF-β1, Collagen I, and α-SMA were significantly increased in Group P compared to Group S ($P < 0.01$). However, treatment with febuxostat significantly suppressed these changes at both the mRNA and protein levels compared to Group P, especially at a dose of 10 mg/kg per day ($P < 0.01$). Furthermore, RAP caused a

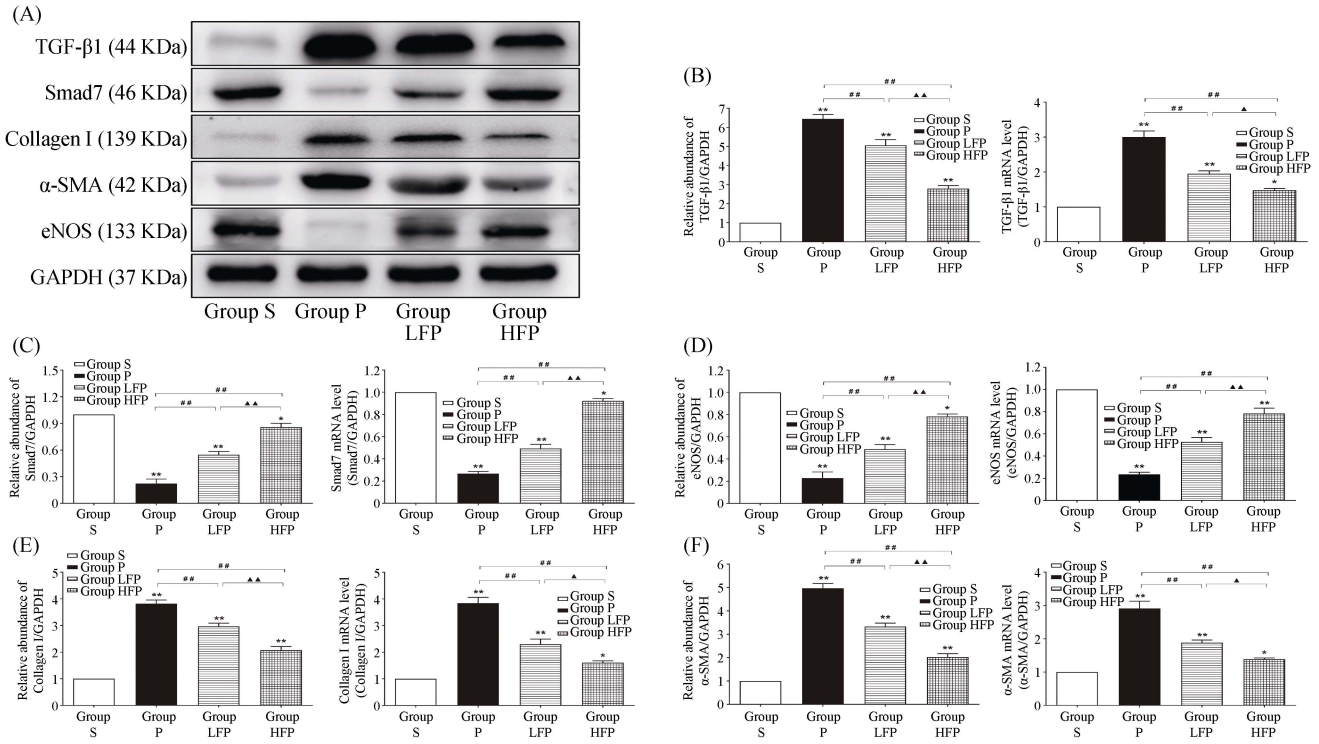

Figure 4. Effects of febuxostat on the expression of TGF-β1, Smad7, eNOS, Collagen I, and α-SMA in the left atrium. (A): Western blot analysis of the protein expression levels of TGF-β1, Smad7, eNOS, Collagen I, and α-SMA in samples from Group P, Group S, Group LFP, and Group HFP; (B): quantitative analysis of the mRNA and protein expression levels of TGF-β1; (C): quantitative analysis of the mRNA and protein expression levels of Smad7; (D): quantitative analysis of the mRNA and protein expression levels of eNOS; (E): quantitative analysis of the mRNA and protein expression levels of Collagen I; and (F): quantitative analysis of the mRNA and protein expression levels of α-SMA. Values are expressed as means ± SD (n = 6/group); $^{*}P < 0.05$ and $^{**}P < 0.01$ *vs*. Group S; $^{\#}P < 0.05$ and $^{\#\#}P < 0.01$ *vs*. Group P; $^{\blacktriangle}P < 0.05$ and $^{\blacktriangle\blacktriangle}P < 0.01$ *vs*. Group LFP. Group S: sham-operated group; Group P: RAP group; Group LFP: RAP with 5 mg/kg per day febuxostat group; Group HFP: RAP with 10 mg/kg per day febuxostat group. RAP: rapid atrial pacing.

significant decrease in the expression of Smad7 and eNOS in Group P compared to Group S ($P < 0.01$). By contrast, the mRNA and protein levels of Smad7 and eNOS were higher in the febuxostat-treated groups than those in Group P ($P < 0.01$).

4 Discussion

This study showed that four weeks of RAP in a rabbit model induced oxidative stress injury, inflammatory reactions, and atrial electrical and structural remodeling. Febuxostat treatment inhibited this RAP-induced oxidative stress and inflammation and attenuated the development of atrial electrical and structural remodeling. Moreover, febuxostat treatment ameliorated atrial fibrosis and atrial structure remodeling induced by RAP by modulating the TGFβ1/Smad signal transduction pathway.

Atrial electrical remodeling is characterized by ion channel dysfunction, which can result in substrate re-entry.[24] Previous studies have demonstrated that after the onset of AF, AERP becomes shorter, and the physiological effective refractory period (ERP) rate adaptation is reduced.[23,25] AERP shortening makes it much easier to find excitable tissue in a potential re-entry circuit and leads to AF perpetuation.[26] Atrial tachycardia directly induces Ca^{2+} accumulation by increasing the frequency of action potentials, during which depolarization-induced calcium currents carry Ca^{2+} into atrial myocytes.[25] High-atrial-rate-induced intracellular Ca^{2+} overload is prevented by short- and long-term adaptations that reduce Ca^{2+} entry at the expense of decreases in the duration of atrial action potential (APD), which results in increased vulnerability to AF through shortening of AERP.[27] The downregulation of L-type calcium channels and transient outward potassium channels caused by Ca^{2+} overload plays a key role in atrial tachycardia-induced ionic current remodeling, and it is an important factor in the occurrence and maintenance of AF.[28] The results of this study partially verify this mechanism. The observed electrophysiological changes—for example, the decrease in AERP200 and the increase in AF inducibil-

ity—are consistent with the downregulation of Cav1.2 and Kv4.3 mRNA in Group P compared to Group S. This is also consistent with previous studies that used different animal models of AF.[29,30] As demonstrated in this study, atrial electrical remodeling alters the ionic currents and gene expression of ion channels, which produces a substrate favorable for AF and promotes the occurrence of AF.

Atrial structural remodeling is characterized by atrial enlargement and interstitial fibrosis, and it is considered a major contributor to AF.[4] In animal models of RAP-induced AF, electrical remodeling can be reversed by the termination of RAP; however, this remodeling cannot be reversed in the presence of atrial fibrosis.[31] In this study, echocardiography revealed LA enlargement and dysfunction following four weeks of RAP, and H&E staining revealed that the left atrial tissue had serious pathological damage. Moreover, Masson's trichrome staining showed that the proportion of fibrous tissue was significantly higher, and transmission electron microscopy revealed significant deposition of collagen fibers. All of these effects were reversed by treatment with febuxostat, demonstrating that febuxostat has cardio-protective effects and that treatment with febuxostat attenuates the development of atrial electrical and structural remodeling in a rabbit model of AF induced by RAP.

Many studies have shown that atrial remodeling is promoted by inflammation and oxidative stress, as evidenced by changes in inflammatory and oxidative stress markers during AF.[5,6] hs-CRP has been identified as the most common inflammatory marker in this situation, and it has proven to be a strong predictor of the current presence, future development, and recurrence of AF.[32] GDF-15 is emerging as a novel inflammatory marker in the cardiovascular system, and it has been shown to be a potential prognostic biomarker in patients with heart failure, acute coronary syndrome, acute pulmonary embolism, and paroxysmal AF.[33] Our results show that hs-CRP and GDF-15 levels were clearly elevated in the serum of Group P animals compared with those in Group S, indicating that four weeks of RAP induced a severe inflammatory response. However, treatment with febuxostat, especially at a dose of 10 mg/kg per day, significantly decreased levels of hs-CRP and GDF-15, indicating that febuxostat attenuated the RAP-induced inflammatory response. SOD, XO, and XDH are important indicators of oxidative stress. RAP for four weeks induced a decrease in SOD activity and an increase in XO and XDH activities. Treatment with febuxostat attenuated the decrease in SOD activity and the increase in XO and XDH activities, suggesting that febuxostat reduced RAP-induced oxidative stress by inhibiting XOR. Uncoupled NOS is one of the primary sources of ROS in atrial tissues.[8] In this study, we found that RAP caused a significant reduction in the mRNA and protein expression levels of eNOS. The inhibition of eNOS production can result in an increase in ROS generation, which can promote atrial remodeling. In addition, febuxostat treatment resulted in the upregulation of eNOS induced by RAP. Galectin-3 is a profibrotic molecule that plays a role in cardiac structural remodeling.[34] Serum galectin-3 level is independently correlated with the extent of LA fibrosis, as demonstrated by Delayed Enhancement Magnetic Resonance Imaging (DE-MRI) of paroxysmal AF patients with preserved LV function.[35] In this study, we found that the level of serum galectin-3 was significantly increased in Group P compared to those in Group S, and febuxostat treatment resulted in a smaller increase in galectin-3 level. Taken together, these results suggest that febuxostat may prevent atrial electrical and structural remodeling in response to RAP by attenuating inflammatory responses and oxidative stress injury by inhibiting XO.

The pathogenesis of AF and the molecular mechanisms underlying the protective effects of febuxostat are still poorly understood. Gramley, *et al*.[36] demonstrated that atrial fibrogenesis in patients with AF is associated with changes in TGF-β1. These changes in TGF-β1 during the establishment of AF provide the opportunity to selectively interfere with the atrial remodeling process at different stages. Recent studies have indicated that TGF-β1, which acts through the Smad signaling pathway to stimulate collagen production, is central to signaling cascades implicated in the genesis of cardiac fibrosis.[37,38] TGF-β1 exhibits its profibrotic impact primarily through phosphorylated (p-) Smad2/3, while Smad7 inhibits TGF-β1 signaling.[36,39] In this study, we found that RAP induced a significant increase in the expression of TGF-β1 and a significant decrease in the expression of Smad7, resulting in a marked increase in both α-SMA and collagen I synthesis. α-SMA is a phenotypic marker of myofibroblasts, and the expression of SMA is positively correlated with atrial fibrosis.[38] The increased expression of α-SMA and collagen I further confirms that RAP is associated with more severe atrial structural remodeling. Therefore, we assumed that the cardio-protective effects of febuxostat on atrial structural remodeling were due in large part to the downregulation of TGF-β1 and the inhibition of the TGF-β1/Smad signaling pathway. Our results support the assumption that treatment with febuxostat results in a decrease in the expression of TGF-β1, which eventually leads to a reduction in atrial fibrosis.

Febuxostat is a potent XO inhibitor used in the treatment of hyperuricemia in patients with gout.[17] In contrast to allopurinol, febuxostat can selectively inhibit XO without

cross-inhibiting other enzymes involved in purine and pyrimidine metabolism, and it is better tolerated by patients with renal dysfunction.[40] It is interesting that the recent Cardiovascular Safety of Febuxostat and Allopurinol in Patients with Gout and Cardiovascular Morbidities (CARES) trial on the cardiovascular risk of febuxostat versus that of allopurinol showed that the individual risk of cardiovascular mortality and all-cause mortality were 1.2 to 1.3 times higher with febuxostat than with allopurinol.[41] This clinical trial has raised questions about the cardiovascular safety of febuxostat. The results of this clinical trial seem to be inconsistent with the results presented in this study. We suppose that in rabbits, and perhaps in humans, the inhibition of XO activity and the associated oxidative stress and inflammation upon treatment with febuxostat may only be of therapeutic benefit during the initial phases of atrial remodeling and cardiac functional deterioration. However, once atrial enlargement and atrial fibrosis were established, XO inhibition would no longer offer any significant protective effects.

4.1 Limitations

Our animal study had certain limitations. First, febuxostat was not previously investigated as a treatment for AF, so the doses used in this study were selected based on clinical studies for the treatment of hyperuricemia in patients with gout. Further animal experiments and clinical trials will be needed to determine the optimal dosage and the frequency of febuxostat treatments. Second, although this study demonstrated that TGF-β1 can mediate atrial fibrosis through the Smad signaling pathway, we cannot exclude the possibility that TGF-β1 may have other mediators that participate in the fibrotic process. These issues need to be explored in future studies.

4.2 Conclusions

This study is the first to find that febuxostat can inhibit atrial electrical and structural remodeling of AF induced by RAP. It could be a potential anti-atrial fibrillation drug owing to its attenuation of inflammation and oxidative stress by suppressing XO and inhibiting the TGF-β1/Smad signaling pathway. Although further studies are needed before clinical application, febuxostat may be potentially useful as a novel upstream therapy in the treatment of AF.

Acknowledgment

This study was supported by the Beijing Natural Science Foundation (Z141100002114050). There was no conflict of interests to be declared.

References

1 Lip GY, Tse HF, Lane DA. Atrial fibrillation. *Lancet* 2012; 379: 648–661.
2 Woods CE, Olgin J. Atrial fibrillation therapy now and in the future: drugs, biologicals, and ablation. *Circ Res* 2014; 114: 1532–1546.
3 Lau DH, Linz D, Schotten U, *et al*. Pathophysiology of paroxysmal and persistent atrial fibrillation: rotors, foci and fibrosis. *Heart Lung Circ* 2017; 26: 887–893.
4 Jalife J, Kaur K. Atrial remodeling, fibrosis, and atrial fibrillation. *Trends Cardiovasc Med* 2015; 25: 475–484.
5 Harada M, Van Wagoner DR, Nattel S. Role of inflammation in atrial fibrillation pathophysiology and management. *Circ J* 2015; 79: 495–502.
6 Zakkar M, Ascione R, James AF, *et al*. Inflammation, oxidative stress and postoperative atrial fibrillation in cardiac surgery. *Pharmacol Ther* 2015; 154: 13–20.
7 Zhao Z, Ng CY, Liu T, *et al*. Relaxin as novel strategy in the management of atrial fibrillation: potential roles and future perspectives. *Int J Cardiol* 2014; 171: e72–e73.
8 Pinho-Gomes AC, Reilly S, Brandes RP, Casadei B. Targeting inflammation and oxidative stress in atrial fibrillation: role of 3-hydroxy-3-methylglutaryl-coenzyme a reductase inhibition with statins. *Antioxid Redox Signal* 2014; 20: 1268–1285.
9 Dudley SC Jr., Hoch NE, McCann LA, *et al.* Atrial fibrillation increases production of superoxide by the left atrium and left atrial appendage: role of the NADPH and xanthine oxidases. *Circulation* 2005; 112: 1266–1273.
10 Korantzopoulos P, Letsas KP, Liu T. Xanthine oxidase and uric Acid in atrial fibrillation. *Front Physiol* 2012; 3: 150.
11 Hou M, Hu Q, Chen Y, et al. Acute effects of febuxostat, a non-purine selective inhibitor of xanthine oxidase, in pacing induced heart failure. *J Cardiovasc Pharmacol* 2006; 48: 255–263.
12 Lee TM, Lin SZ, Chang NC. Effects of urate-lowering agents on arrhythmia vulnerability in post-infarcted rat hearts. *J Pharmacol Sci* 2016; 131: 28–36.
13 Li Y, Chen F, Deng L, *et al.* Febuxostat attenuates paroxysmal atrial fibrillation-induced regional endothelial dysfunction. *Thromb Res* 2017; 149: 17–24.
14 Sakabe M, Fujiki A, Sakamoto T, *et al*. Xanthine oxidase inhibition prevents atrial fibrillation in a canine model of atrial pacing-induced left ventricular dysfunction. *J Cardiovasc Electrophysiol* 2012; 23: 1130–1135.
15 Day RO, Kamel B, Kannangara DR, *et al*. Xanthine oxidoreductase and its inhibitors: relevance for gout. *Clin Sci (Lond)* 2016; 130: 2167–2180.
16 Chen C, Lu JM, Yao Q. Hyperuricemia-related diseases and Xanthine Oxidoreductase (XOR) Inhibitors: an overview. *Med Sci Monit* 2016; 22: 2501–2512.
17 Ernst ME, Fravel MA. Febuxostat: a selective xanthine-oxidase/xanthine-dehydrogenase inhibitor for the management of hyperuricemia in adults with gout. *Clin Ther* 2009; 31: 2503–2518.

18 Wang S, Li Y, Song X, *et al.* Febuxostat pretreatment attenuates myocardial ischemia/reperfusion injury via mitochondrial apoptosis. *J Transl Med* 2015; 13: 209.
19 Saban-Ruiz J, Alonso-Pacho A, Fabregate-Fuente M, *et al*. Xanthine oxidase inhibitor febuxostat as a novel agent postulated to act against vascular inflammation. *Antiinflamm Antiallergy Agents Med Chem* 2013; 12: 94–99.
20 Krishnamurthy B, Rani N, Bharti S, *et al.* Febuxostat ameliorates doxorubicin-induced cardiotoxicity in rats. *Chem Biol Interact* 2015; 237: 96–103.
21 Omori H, Kawada N, Inoue K, *et al.* Use of xanthine oxidase inhibitor febuxostat inhibits renal interstitial inflammation and fibrosis in unilateral ureteral obstructive nephropathy. *Clin Exp Nephrol* 2012; 16: 549–556.
22 Shafik AN. Febuxostat improves the local and remote organ changes induced by intestinal ischemia/reperfusion in rats. *Dig Dis Sci* 2013; 58: 650–659.
23 Zhang DX, Ren K, Guan Y, *et al*. Protective effects of apocynin on atrial electrical remodeling and oxidative stress in a rabbit rapid atrial pacing model. *Chin J Physiol* 2014; 57: 76–82.
24 Nattel S, Harada M. Atrial remodeling and atrial fibrillation: recent advances and translational perspectives. *J Am Coll Cardiol* 2014; 63: 2335–2345.
25 Sun H, Chartier D, Leblanc N, Nattel S. Intracellular calcium changes and tachycardia-induced contractile dysfunction in canine atrial myocytes. *Cardiovasc Res* 2001; 49: 751–761.
26 Staerk L, Sherer JA, Ko D, *et al*. Atrial fibrillation: epidemiology, pathophysiology, and clinical outcomes. *Circ Res* 2017; 120: 1501–1517.
27 Denham NC, Pearman CM, Caldwell JL, *et al.* Calcium in the pathophysiology of atrial fibrillation and heart failure. *Front Physiol* 2018; 9: 1380.
28 Qi XY, Yeh YH, Xiao L, *et al.* Cellular signaling underlying atrial tachycardia remodeling of L-type calcium current. *Circ Res* 2008; 103: 845–854.
29 Zhao Y, Gu TX, Zhang GW, *et al*. Losartan affects the substrate for atrial fibrillation maintenance in a rabbit model. *Cardiovasc Pathol* 2013; 22: 383–388.
30 Li Y, Li W, Yang B, *et al.* Effects of Cilazapril on atrial electrical, structural and functional remodeling in atrial fibrillation dogs. *J Electrocardiol* 2007; 40: 100 e101–e106.
31 Allessie M, Ausma J, Schotten U. Electrical, contractile and structural remodeling during atrial fibrillation. *Cardiovasc Res* 2002; 54: 230–246.
32 Chung MK, Martin DO, Sprecher D, *et al.* C-reactive protein elevation in patients with atrial arrhythmias: inflammatory mechanisms and persistence of atrial fibrillation. *Circulation* 2001; 104: 2886–2891.
33 Shao Q, Liu H, Ng CY, *et al.* Circulating serum levels of growth differentiation factor-15 and neuregulin-1 in patients with paroxysmal non-valvular atrial fibrillation. *Int J Cardiol* 2014; 172: e311–e313.
34 Hernandez-Romero D, Vilchez JA, Lahoz A, *et al.* Galectin-3 as a marker of interstitial atrial remodelling involved in atrial fibrillation. *Sci Rep* 2017; 7: 40378.
35 Yalcin MU, Gurses KM, Kocyigit D, *et al.* The Association of Serum Galectin-3 Levels with Atrial Electrical and Structural Remodeling. *J Cardiovasc Electrophysiol* 2015; 26: 635–640.
36 Gramley F, Lorenzen J, Koellensperger E, *et al*. Atrial fibrosis and atrial fibrillation: the role of the TGF-beta1 signaling pathway. *Int J Cardiol* 2010; 143: 405–413.
37 Mira YElA, Muhuyati, Lu WH, *et al*. TGF-β1 signal pathway in the regulation of inflammation in patients with atrial fibrillation. *Asian Pac J Trop Med* 2013; 6: 999–1003.
38 Lugenbiel P, Wenz F, Govorov K, *et al*. Atrial myofibroblast activation and connective tissue formation in a porcine model of atrial fibrillation and reduced left ventricular function. *Life Sci* 2017; 181: 1–8.
39 He X, Gao X, Peng L, *et al.* Atrial fibrillation induces myocardial fibrosis through angiotensin II type 1 receptor-specific Arkadia-mediated downregulation of Smad7. *Circ Res* 2011; 108: 164–175.
40 Zhao L, Roche BM, Wessale JL, *et al.* Chronic xanthine oxidase inhibition following myocardial infarction in rabbits: effects of early versus delayed treatment. *Life Sci* 2008; 82: 495–502.
41 White WB, Saag KG, Becker MA, *et al.* Cardiovascular Safety of Febuxostat or Allopurinol in Patients with Gout. *N Engl J Med* 2018; 378: 1200–1210.